

Quantitative electrostatic force measurement in AFM

Steve Jeffery^{*}, Ahmet Oral, John B. Pethica

Department of Materials, University of Oxford, Parks Road, Oxford OX1 3PH, UK

Abstract

We describe a method for measuring forces in the atomic force microscope (AFM), in which a small amplitude oscillation ($\sim 1 \text{ \AA}_{p-p}$) is applied to a stiff ($\sim 40 \text{ N/m}$) cantilever below its first resonant frequency, and the force gradient is measured directly as a function of separation. We have used this instrument to measure electrostatic forces by applying an ac voltage between the tip and the sample, and observed a variation in contact potential difference with separation. We also show how the benefits of this instrument may be exploited to make meaningful capacitance measurements, especially at small tip–surface separations, and demonstrate the potential of this technique for quantitative dopant profiling in semiconductors. © 2000 Elsevier Science B.V. All rights reserved.

Keywords: Amplitude oscillation; Electrostatic force; AFM

1. Introduction

Large amplitude resonant ac mode force microscopy has attracted much attention for high spatial resolution force measurements [1]. Analysing the data to understand the tip–surface interaction has proved to be more difficult, since the amplitudes used are generally much greater than the interaction range. While satisfactory results may be obtained for well-defined, single-valued potentials, there are serious problems for more complex systems, particularly where electrostatic forces are present, as in the present paper.

For semiconductors, the local electrical dissipation [2], the non-uniform distributions of electrical

charge, and the complicated variation of capacitance with voltage make it highly desirable to use a small oscillation amplitude so that the force can be directly measured as a function of separation. In this paper, we demonstrate that such measurements can be made. We find that quantitative imaging and analysis of semiconductors can be carried out, but that very careful characterisation of the processes that would contribute to the total tip–surface force is required.

2. Experimental

In our experiments, a stiff ($k \approx 40 \text{ N/m}$) cantilever is used (obtained from Nanosensors, Germany), and a small oscillation (amplitude $A \approx 1 \text{ \AA}_{p-p}$) is applied at 3.34 kHz, well below the first resonant frequency of the cantilever ($\sim 200 \text{ kHz}$). This oscillation can be applied either to the base of the cantilever using a piezoelectric biomorph, or by coating the reverse side of the cantilever with a thin

^{*} Corresponding author. Tel.: +44-1865-273788; fax: +44-1865-273789.

E-mail address: stephen.jeffery@materials.ox.ac.uk (S. Jeffery).

film of a magnetic material and applying an oscillating magnetic field. The cantilever displacement is measured using a highly sensitive fibre optic interferometer (noise level $< 5 \times 10^{-4} \text{ \AA}/\sqrt{\text{Hz}}$), in which an interference cavity is formed between the end of the fibre and the back of the lever. The relevant frequency component of the motion is measured using a lock-in amplifier. When the tip is brought close to the surface, the tip–surface interaction alters the effective stiffness of the cantilever, thus changing the oscillation amplitude. For both methods of tip modulation, the tip–surface force gradient k_{t-s} is related to the oscillation amplitude A by [3]:

$$k_{t-s} = k \left(\frac{A_0}{A} - 1 \right) \quad (1)$$

where k is the lever stiffness and A_0 the amplitude far from the surface. This simple model allows us to measure the variation of k_{t-s} with tip–surface separation z quantitatively, without making any assumptions about the tip–surface force other than that it is linear over the range of the cantilever oscillation amplitude. The true $F-z$ curve is then found by integration. A similar technique to this has been employed in the past [4]. The important difference between this technique and other small-amplitude methods [3,5,6], is that we use a relatively stiff cantilever, which prevents snap-in without the need for feedback control of the dc component of the applied force. This is possible because of the high sensitivity of our interferometric displacement sensor.

An important experimental point is that the magnetic oscillation method [4] gave less consistent results than piezoelectric modulation. This was probably because the modes of motion caused by the magnetic modulation were rather complex; indeed, such complex motions could readily be observed by moving the end of the optical fibre over the surface of the lever. For this reason, we use piezoelectric modulation in most of our experiments, although we envisage that the magnetic oscillation technique could be improved by carefully controlling the magnetisation of the film.

In order to measure electrostatic forces, we applied a voltage $V = V_{dc} + V_{ac} \sin(\omega t)$ between the tip

and the sample, which gives rise to an electrostatic force given by [7]:

$$\begin{aligned} F_e = & \frac{1}{2} \left(\left(V_{dc} + \frac{\Delta\phi}{e} \right) + \frac{1}{2} V_{ac}^2 \right) \frac{dC}{dz} \\ & + \frac{1}{2} V_{ac} \left(V_{dc} + \frac{\Delta\phi}{e} \right) \frac{dC}{dz} \sin(\omega t) \\ & + \frac{1}{4} V_{ac}^2 \frac{dC}{dz} \cos(2\omega t) \end{aligned} \quad (2)$$

C is the tip–sample capacitance, ω is the frequency, and $(\Delta\phi)/e$ is the contact potential difference (CPD). We denote the separate frequency components of this force by F_{dc} , F_{ω} and $F_{2\omega}$. We measure the individual components of the electrostatic force separately using a lock-in amplifier, which allows us to distinguish electrostatic interactions from other interactions, and to gain extra information about the sample.

The probe was coated with a 10-nm chromium layer and a 30-nm gold layer by evaporation. The thermal drift in our experiments is reduced to a low level (a few angstrom per minute) by enclosing the instrument in a heavy cabinet and allowing the temperature to stabilise before performing experiments. Lock-in time constants between 100 and 500 ms were used, the precise values being determined by the amplitude and time variation of the signal.

3. Results and discussion

We recall that the electrostatic force $F_{2\omega}$ is influenced by the electrical properties of the sample in the region of the tip via the total capacitance C of the tip–surface junction. This provides a means of measuring the local sample properties. However, C is also influenced by purely geometrical factors, such as the shape of the tip. Clearly, before we can examine the effect of the sample properties on $F_{2\omega}$, we must understand the effect of these geometrical factors. For this, we require a sample which itself contributes negligibly to the total capacitance, so that the dominant contribution comes from the tip–surface gap.

We therefore performed $F-z$ measurements on a gold sample using a gold-coated probe with $V_{ac} = 10$

V , $V_{dc} = 0$ V, and $\omega = 10.35$ kHz. We found that the amplitude of $F_{2\omega}$ did not decrease rapidly to zero at large separations as we had initially expected. Instead, there was a significant long-range background force, which was found to be present even at separations of several micrometers. This long-range component is clearly important, and arises from the electrostatic force on the more remote regions of the tip and the main body of the cantilever.

We devised a simple electrostatic model to fit the measured data, and we found that the predictions of the model depended extremely and strongly on the assumed geometry of the probe. It was not sufficient to use a simple model for the tip, such as a sphere or a truncated cone; instead, the experimental results could only be adequately explained by taking into account the actual micrometer-scale shape of the tip, and the shape and tilt angle of the cantilever. This would add complications to any realistic quantitative model of the electrostatic force, although these macroscopic effects obviously become less important at very small separations.

We then performed a series of measurements on a thermally oxidised n-type Si wafer (oxide thickness = 70 Å, doping level $\approx 10^{15}$ cm $^{-3}$), in which we measured the variation of F_{ω} with z at different values of V_{dc} . With Eq. 2 in mind, the results we obtained at large positive and negative values of V_{dc} were fairly predictable. The amplitude of F_{ω} increased with decreasing z , being greater at the larger values of V_{dc} , and the phase of F_{ω} changed by 180° when the sign of V_{dc} was reversed, indicating a change in sign of $V_{dc} + (\Delta\phi)/e$. However, at small values of V_{dc} , an unexpected effect was observed, which is shown in Fig. 1. Within a small range of values of V_{dc} , F_{ω} initially decreased in amplitude with decreasing z , then went through zero, changed in phase by 180° , and began to increase once again.

We had expected that the amplitude of F_{ω} would simply decrease as V_{dc} was brought closer to balancing the CPD (i.e., as $V_{dc} + (\Delta\phi)/e$ became small), and that it would be zero at a single value of V_{dc} (the so-called ‘Kelvin null voltage’ [7]) for all values of z . However, our results indicate that, although a ‘null’ does occur, it occurs over a range of values of V_{dc} , each corresponding to a single unique value of separation. In other words, the apparent CPD is dependent on separation, and varied by several hun-

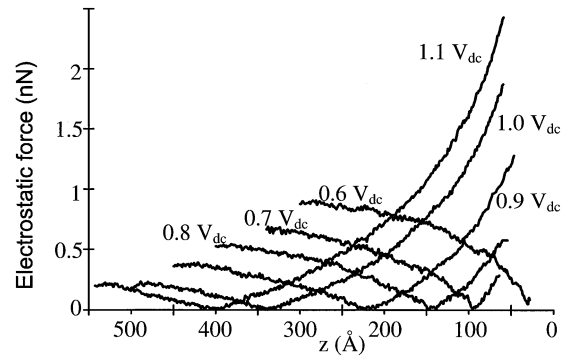


Fig. 1. $F-z$ curves showing the amplitude of F_{ω} on a silicon sample, with $V_{ac} = 4$ V $_{p-p}$ at different values of V_{dc} . Approach rate = 0.5 Å/s. The phase of F_{ω} changes by 180° as it passes through the ‘null’ point, indicating a change in the sign of $V_{dc} + (\Delta\phi)/e$. These data demonstrate that the CPD is not characterised by a single value independently of separation.

dred millivolts with this sample as the separation was changed by a few hundred angstroms.

One possible explanation of these results is that there are spatial variations in CPD, due to compositional inhomogeneities, contaminants, etc. (these experiments were carried out in air), as well as fixed charge near the surface. As a result of these spatial variations, different regions of the tip–surface junction would experience different electrostatic stress (i.e., electrostatic force per unit area) depending on the actual CPD at that location, and the local probe–surface separation. As the separation is varied, the size of the contributions from the different parts of the tip–surface junction changes, resulting in a gradual change in average CPD with separation. Another possible explanation is that there may be mobile surface charges, which can only move slowly, on a time scale comparable with the period of the ac voltage signal. The charge distribution would then not reach equilibrium, and any change in the tip–surface separation would change the length scale of the charge motion induced.

These results have important implications for interpretation of CPD measurements made with conventional Kelvin probe force microscopy and similar techniques, particularly if large oscillation amplitudes are used.

We carried out a further series of measurements on this sample, in which we measured the variation of $F_{2\omega}$ with separation at different values of V_{dc} . As

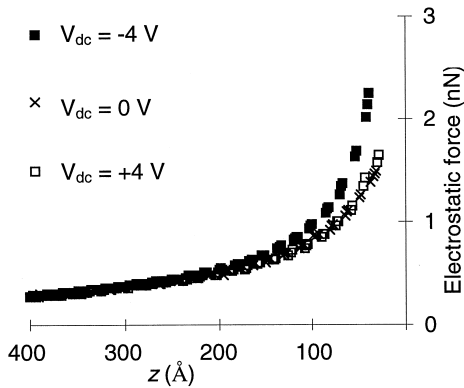


Fig. 2. $F-z$ curves showing the RMS amplitude of $F_{2\omega}$ on an n-type silicon sample with $V_{ac} = 4 V_{p-p}$. Approach rate = 3 \AA/s . The values of $V_{dc} = -4$ and $+4 \text{ V}$ correspond to accumulation and depletion, respectively. These data are therefore in qualitative agreement with the expected behaviour of a metal-insulator-semiconductor capacitor, in which the capacitance is greater under accumulation than depletion.

mentioned previously, these measurements provide information about the sample properties via the total capacitance gradient $(dC)/(dz)$ of the tip-surface junction (Eq. 2). With this sample, we expect two major contributions to the sample capacitance, from the oxide film and from the substrate, the latter contribution being dependent on V_{dc} . It can clearly be seen in Fig. 2 that the amplitude of $F_{2\omega}$ is greater at small separations with $V_{dc} = -4 \text{ V}$ (accumulation) than with $V_{dc} = +4 \text{ V}$ (depletion) or $V_{dc} = 0 \text{ V}$. This is in qualitative agreement with a simple model in which the contributions to the capacitance from the tip-surface gap and the sample are added in series [7], since we expect the sample capacitance under depletion to be significantly lower than that under accumulation.

As mentioned previously, a major motivation for work of this kind is quantitative imaging of 2-D dopant density variations in semiconductors. Our aim would be to produce data of the kind shown in Fig. 2 for each of the different regions of the sample. There are at least two possible approaches to this task in our atomic force microscope (AFM). The first is to use the amplitude of the piezo-driven oscillation as the feedback signal, thereby tracing contours of constant force gradient, and simultaneously measure $F_{2\omega}$. We obtained a number of images in this way, of both surface topography and variations in dopant

density. However, one slight problem with this technique is that there is a change in the slope of k_{t-s} with z at small separations, so the feedback loop can be rather unstable. As a result, a long time constant (several hundred milliseconds) must be used in the lock-in amplifier in order to improve the signal-to-noise ratio, and a low feedback gain must therefore be used, so imaging becomes rather slow.

An alternative approach, which permits faster imaging, is to use $F_{2\omega}$ as the feedback signal. In this scheme, the slope of the feedback signal with z is higher (giving a higher gain), and has the same sign over a larger z range (improving the stability). Both of these factors allow images to be scanned more quickly, with scan speeds of around $1 \mu\text{m s}^{-1}$. The tip then traces contours of constant $F_{2\omega}$, effectively taking ‘slices’ through the $F-z$ curves at different parts of the sample. By generating a number of images at different values of $F_{2\omega}$, $F-z$ curves can be generated for each of the different regions of the sample. Using this approach, we produced a number of images of a VLSI test structure, such as the one shown in Fig. 3. This sample consists of an n-type silicon wafer with an array of heavily implanted p-type regions at the surface. From these images, and having measured an $F-z$ curve on the p-type region

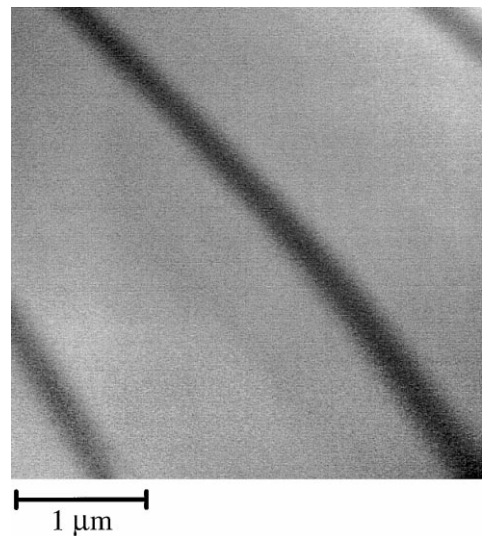


Fig. 3. Image of a silicon VLSI test structure obtained using $F_{2\omega}$ as the feedback signal; $3.8\text{-}\mu\text{m}$ scan. The bright regions are highly doped p-type; the dark regions are low doped n-type. The greyscale range is $\sim 15 \text{ \AA}$.

of the surface to provide a reference, we generated a number of points on the $F-z$ curve for the n-type region. Clearly, the advantage of this technique over simply measuring multiple $F-z$ curves is greater when a large number of different regions are present. The $F-z$ curves so produced could, in principle, be used to extract accurate values of C_s provided that the geometrical effects described above are properly accounted for.

The spatial resolution of this technique is likely to be comparable with that of the other similar techniques [7], since it is determined largely by the tip–surface geometry and the range of the forces involved. However, it is possible that our method may provide higher resolution than some of the other approaches, due to the smaller stable tip–surface separations accessible with the stiff cantilevers used.

4. Conclusion

We have described a small-amplitude technique for making quantitative force measurements in the AFM. We have used this instrument to measure electrostatic forces for the first time, and observed a previously unreported variation in CPD with separa-

tion. In addition, we have shown how local capacitance measurements can be made, and demonstrated its application to dopant profiling in semiconductors.

Acknowledgements

We are grateful to D. F. Ogletree for useful discussions.

References

- [1] U. Dürig, *Appl. Phys. Lett.* 73 (1999) 433, and references therein.
- [2] W. Denk, D.W. Pohl, *Appl. Phys. Lett.* 59 (1991) 2171.
- [3] S.J. O'Shea, M.E. Welland, J.B. Pethica, *Chem. Phys. Lett.* 223 (1994) 336.
- [4] S.P. Jarvis, M.A. Lantz, U. Dürig, H. Tokumoto, *Appl. Surf. Sci.* 140 (1999) 309.
- [5] S.P. Jarvis, H. Yamada, S.-I. Yamamoto, H. Tokumoto, *Rev. Sci. Instrum.* 67 (1996) 2281.
- [6] S.P. Jarvis, H. Yamada, S.-I. Yamamoto, H. Tokumoto, J.B. Pethica, *Nature* 384 (1996) 247.
- [7] T. Hochwitz, A.K. Henning, C. Levey, C. Daghlian, J. Slinkman, J. Never, P. Kaszuba, R. Gluck, R. Wells, J. Pekarik, R. Finch, *J. Vac. Sci. Technol., B* 14 (1996) 440.